Physica A 391 (2012) 4727–4739

Contents lists available at SciVerse ScienceDirect

Physica A

journal homepage: www.elsevier.com/locate/physa

The time-singularity multifractal spectrum distribution

Gang Xiong [a,*], Shuning Zhang [a], Qiang Liu [b]

[a] Electronic engineering department, Nanjing University of Science and Technology, Nanjing, 210094, China

[b] Department of Campaign and Tactical, Air Defense Forces Academy, Zhengzhou, 450052, China

ARTICLE INFO

Article history:
Received 14 September 2011
Received in revised form 18 January 2012
Available online 26 May 2012

Keywords:
Multifractal singularity spectrum
Wavelet transform module maxima method
Non-stationary signal processing
Time-series analysis

ABSTRACT

Although the multifractal singularity spectrum revealed the distribution of singularity exponent, it failed to consider the temporal information, therefore it is hard to describe the dynamic evolving process of non-stationary and nonlinear systems. In this paper, we aim for a multifractal analysis and propose a time-singularity multifractal spectrum distribution (TS-MFSD), which will hopefully reveal the spatial dynamic character of fractal systems. Similar to the Wigner–Ville time-frequency distribution, the time-delayed conjugation of fractal signals is selected as the windows function. Furthermore, the time-varying Holder exponent and the time-varying wavelet singularity exponent are deduced based on the instantaneous self-correlation fractal signal. The time-singularity exponent distribution i.e. TS-MFSD is proposed, which involves time-varying Hausdorff singularity spectrum distribution, time-varying large deviation multifractal spectrum and time-varying Legendre spectrum distribution, which exhibit the singularity exponent distribution of fractal signal at arbitrary time. Finally, we studied the algorithm of the TS-MFSD based on the wavelet transform module maxima method, analyzed and discussed the characteristic of TS-MFSD based on Devil Staircase signal, stochastic fractional motion and real sea clutter.

1. Introduction

Frequently, complex natural systems present characteristics of scalar invariance and fractal behavior that has been verified experimentally and studied theoretically during the past years. There exists a very rich bibliography about fractal and multifractal theory and its application that was reported from very diverse fields as those belonging to physics, ecology, biology, economy, chemistry and math [1–6].

Since the 1960's, the development of fractals theory have gone through *three stages*. *The first stage is the progress from no order to fractal order, and especially the foundation of fractal theory (FT)* based on the Hausdorff measure and Hausdorff dimension [7,8]. As a new mathematics branch, FT interprets the difficulties, such as the length of the British coastline, the differentiability and continuity of the Weirstrass function, the topology length of a Cantor set and so on, which are regarded as morbid and irregular in traditional math. Furthermore, the applications of FT in signal processing developed fractal signal processing. Researches show fractals are fit for signal modeling in the real world, such as electroencephalograms (EEG), electrocardiograms (ECG), as well as turbulent flows, lightning strikes, DNA sequences, and geographical objects which represent some of many natural phenomena and are difficult to be characterized using traditional signal processing theory [6–8]. Fractal dimension describes the geometry character of a fractal signal, including measurement of the complexity, singularity and irregularity of the signal, whose estimation is the key problem of FT [6]. In the past decades, various definitions and algorithms of global fractal dimension have been proposed through the history for FT, which included

* Corresponding author. Tel.: +86 13761230701; fax: +86 02584315843.
E-mail addresses: honey_xiong@163.com, pdxiong@gmail.com (G. Xiong), shuningzhang0704@163.com (S. Zhang), simith_lq@sina.com (Q. Liu).

0378-4371/$ – see front matter © 2012 Elsevier B.V. All rights reserved.
doi:10.1016/j.physa.2012.05.026

the measure method, the FBM method and the IFS method [7]. Besides the Hausdorff dimension, several global fractal dimensions were brought forward, such as self-similar dimension, box-counting dimension, capacity dimension, padding dimension, Kolmogorov dimension and Lyapunov dimension, and the relationships among those FDs are still a puzzle, while they are all based on the idea of "the measure under the scale δ" [7–9].

The second stage of FT theory is from the global fractal and regular fractal dimension to the local fractal, furthermore the multifractal/singularity spectrum (MFS). The Multifractal Formalism is based on the calculation of two sets of coefficients associated to the signals: the Holder exponents (HE) that quantify the local regularity of a signal or function f and the MFS that quantifies the multifractality of f. The MFS associates each group of data with the same regularity at a given point with the Hausdorff dimension of this set of points. In this way, it defines a function between the HE and the Hausdorff dimension that is also known as a spectrum of singularities [7,8]. So the local HE surveyed the local singularity of the signal, but for the multifractal signal with singularity fluctuating from point to point, HE loses the global singularity analysis of the signal. Multifractality provides mathematical concepts and numerical tools for the description of fluctuations of the regularity of a signal, which is derived from the statistic distribution and scaling properties of the local HIM. As a tool for studying the singularity measure, the application of MF in signal analysis and processing aroused scholars' interest around the world.

Stanley and Ostrowsky (1985) and Pietronero and Tosatti (1986) have been pioneers in the development of this research [9]. The MFS is intimately related with the dimension of widespread fractal based on which Grassberger and Procaccia have published studies widely, in the eighties [10–12]. In 1988, Chhabra and co-workers studied the relationship between the MFS and the entropy density of a fractal system, and related the Holder exponent with the free energy of the fractal set [13,14]. After that, Arneodo and Bacry proposed the Wavelet Transform Modulo Maxima Method (WTMM) [15–17]. In 1995, Peng and collaborators put forward the Detrended Fluctuation Analysis (DFA) [18], proved to adapt the short datasets and having less computational complexity which was successfully applied to the study of sequences of DNA, heartbeat time series, and physiological and economical processes [19–22]. After that, Castro and Moreira introduced the generalization of the DFA, and subsequently, Kantelhardt and Stanley proposed the Multifractal Fluctuation Detrended Analysis (MFDFA) and its application on the non-stationary temporary series analysis with multifractal behavior [23–25]. In the past years, Jaffard with Lashermes and Abry have proposed the Wavelet Leaders (WL) method, a new formulation in terms of the local supreme of the wavelet coefficients or Leaders of the signal. The WL is a new methodology for the characterization of Holder exponents and their relationship between Holder regularity and local oscillations [26–30]. Recently, Schumann and Kantelhardt introduced multifractal centered moving average analysis (MF-CMA) based on the CMA technique and proved that it has even less computational difficulties than MF-DFA [31–33].

The third stage is from MFS theory to short-time multifractal spectrum distribution (ST-MFSD), *and further to time-varying MFS distribution theory*. MFS is the representation and signal transformation from the time domain to the singularity domain, which adapts to the determined signal or stochastic stationary fractal signal. Although the MFS revealed the distribution of the singularity exponent, it failed to consider the temporal information; therefore it is hard to describe the dynamic evolving process of non-stationary and nonlinear systems. As for the determined signal with varied MFS and the non-stationary stochastic fractal signal, Xiong et al. [34] and we [35,36] introduced the windowed MFS, and an analogy to the idea of short-time Fourier analysis, deduced the definition of short-time singularity exponent, and proposed the algorithm of ST-MFSD based on WTMM.

The ST-MFSD method provides the idea and approach of time-varying MFS distribution. Nevertheless, the concept of ideal time-singularity spectrum distribution conflicted with the concept of signal measure at certain time and singularity, which is similar to the time-frequency analysis, where the uncertainty theory does not allow the conception of energy at certain time and frequency, and ideal energy density at certain time and frequency does not exist. Fortunately, we can study the pseudo-energy density and TF structure, to approach the ideal TF analysis. Reassembly, we can approximate the ideal time-singularity distribution according to the research objectives. In Refs. [35,36], we introduced the linear time-singularity spectrum representation. In this paper, we aim to the multifractal analysis and propose time-varying multifractal spectrum distribution (TV-MFSD), which will hopefully reveal the spatial dynamic character of a fractal system.

The rest of this paper is organized as follows. Section 2 is devoted to Time-Singularity Analysis of the instantaneous self-correlation signal. The time-delayed conjugation of analyzed signal is selected as the windows function,and the quadratic time-singularity exponent distribution of the instantaneous self-correlation is deduced. Section 3 proposes the quadratic time-singularity multifractal distribution, which includes Hausdorff measure and singularity spectrum distribution, time-varying large deviation multifractal spectrum and time-varying Legendre spectrum distribution, which exhibit the SE distribution of a signal at an arbitrary time. Section 4 introduces the Wavelet Transform Module Maxima (WTMM) Method of the TS-MFSD as a special form of the Legendre spectrum. In Section 5, we present and discuss the applications and experiment of TS-MFSD based on the Devil's Staircase signal, and finally in Section 6, the conclusion.

2. Time-singularity distribution of the instantaneous self-correlation signal

Reference to the Wigner–Ville time-frequency analysis, the time-delayed conjugation of analyzed signal is selected as the windows function, and the instantaneous self-correlation function is

$$r_{xx}(t,\tau) = E[x*(t+\tau/2)x(t-\tau/2)], \tag{2.1}$$

where * stands for conjugation.

Definition 2.1. A function or the path of a process $x(t)$ is said to be in C_τ^h if there is a polynomial $P_\tau(t)$ such that

$$|r_{xx}(t,u) - P_\tau(u)| \le C|u-\tau|^h \tag{2.2}$$

for u sufficiently close to τ. Then, the local Holder regular degree of $r_{xx}(t,\tau)$ at (t,τ) is $H(t,\tau) := \sup\{h : x(t) \in C_\tau^h\}$. Of special interest for our purpose is the case when the approximating polynomial satisfies $P_\tau(u) = r_{xx}(t,\tau)$, and $H(t,\tau)$ can be computed as follow.

Definition 2.2. Let us agree on the convention $\log(0) = -\infty$ and the time-varying Holder exponent can be described as

$$h(t,\tau) = \liminf_{\varepsilon\to 0} \frac{1}{\log_2(2\varepsilon)} \log_2 \sup_{|u-\tau|<\varepsilon} |r_{xx}(t,\tau) - r_{xx}(t,u)|. \tag{2.3}$$

An essential simplification for both analytical and empirical study is to replace the continuous limit by discrete intervals. To this end we introduce some notation. Let $k_n(\tau) := [\tau 2^n]$, then $k_n(\tau)$ is the unique integer such that $\tau \in I_{kn}^{(n)} := [k_n 2^{-n}, (k_n+1)2^{-n}]$. As n increases the intervals $I_k^{(n)}$ form a nested decreasing sequence. Now, defining a discrete approximation to $h(t,\tau)$, we have to imitate in a discrete manner a ball around τ over which we will consider the increments of $r_{xx}(t,\tau)$. Accounting for the fact that τ could lay very close to the boundary of $I_{kn}^{(n)}$.

Definition 2.3. The coarse Holder exponent of $r_{xx}(t,\tau)$ is

$$h_{kn}^{(n)}(t) := -\frac{1}{n} \log_2 \sup\{|r_{xx}(t,\tau) - r_{xx}(t,u)| : u \in [(k_n-1)2^{-n}, (k_n+2)2^{-n}]\}. \tag{2.4}$$

To compare the limiting behavior of these exponents with $h(t,\tau)$, choose n such that $2^{-n+1} \le \varepsilon \le 2^{-n+2}$, and

$$[(k_n-1)2^{-n}, (k_n+2)2^{-n}] \subset [\tau-\varepsilon, \tau+\varepsilon] \subset [(k_{n-2}-1)2^{-n+2}, (k_{n-2}+2)2^{-n+2}] \tag{2.5}$$

from which it follows immediately that $h(t,\tau) = \liminf_{n\to\infty} h_{kn}^{(n)}(t)$. It is essential to note that the countable set of numbers $h_{kn}^{(n)}(t)$ contains all the scaling information of interest to us. Being defined pathwise, they are random variables.

The definition of $h(t,\tau)$ and $h_{kn}^{(n)}(t)$ is hard to apply to the practice. The study of fine scale properties of functions (as opposed to measures) has been pioneered in the work of Armando, Barry and Muzzy, who were also the first to introduce wavelet techniques in this context. Due to the MRA of WT, wavelet technical possess the particular advantage. According to the tracking and position capability of singularity of WT, the difference of $|r_{xx}(t,\tau) - r_{xx}(t,u)|$ can be replaced by the DWT coefficient, which possess the differential character. Hereby, the time-varying instantaneous wavelet singularity exponent is defined as

Definition 2.4 (*Time-Varying Wavelet Singularity Exponent*)**.** $W_{n,kn}(t)$ is the wavelet coefficient with vanishing moments $n > h(x)$. If $|X(s) - X(t)| = O(|s-t|)^h$ $(s \to t)$ exists,then the time-varying wavelet singularity exponent

$$w(t,\tau) = \liminf_{n\to\infty} w_{kn}^{(n)}(t). \tag{2.6}$$

Where the discrete instantaneous wavelet singularity exponent

$$w_{kn}^{(n)}(t) := -\frac{1}{n} \log_2 |2^{n/2} W_{n,kn}(t)|. \tag{2.7}$$

Note that Definitions 2.2 and 2.3 are in the hypothesis of the signal $r_{xx}(t,\tau)$ can be approximated by the determined polynomial, while the wavelet function possesses the vanishing moments character, i.e.,$\int t^m \varphi(t)dt = 0$, thus wavelet singularity exponent is not influenced by the polynomial variable differential character.

In special applied case, there are also singularity exponents based on probability or other measures. The common ground is power law relationship between the measure and the linear index, and limited calculation and linear imitation.

3. The quadratic time-singularity multifractal spectrum distribution

At the beginning stands the discovery that on fractals local scaling behavior, as measured by exponents $w(t,\tau)$ or $h(t,\tau)$, is not uniform in general. In other words, $w(t,\tau)$ or $h(t,\tau)$ are typically not constant in t and τ, but assume a whole range of values, thus imprinting a rich structure on the object of interest. This structure can be characterized either in geometrical terms making use of the concept of dimension, or in statistical terms based on sample moments. A tight connection between these two descriptions emerges from the multifractal formalism.

As we will see, as far as the validity of the multifractal formalism is concerned there is no restriction in choosing a singularity exponent which seem suited to describing scaling behavior of interest, as long as one is consistent in using the

same exponents for both, the geometrical and the statistical description. To express this fact we consider in this section the arbitrary coarse singularity exponent as $\alpha_{kn}^{(n)}(t)(k = 0, 1, \ldots, 2^n - 1, n \in N)$, which may be any sequence of random variables. To keep a connection with what was said before think of $\alpha_{kn}^{(n)}(t)$ as representing a coarse singularity exponent related to the oscillations over the dyadic interval $I_{kn}^{(n)}$. To accommodate processes which are constant over some intervals we explicitly allow $\alpha_{kn}^{(n)}(t)$ to take the value ∞.

In Section 2, one has the time-varying wavelet singularity exponent matrix. To obtain the singularity distribution in t, we study the quadratic time-singularity multifractal spectrum distribution $f(t, a)$. As for estimation algorithm of $f(t, a)$, there are three kinds of method, respectively, time varying Hausdorff singularity spectrum $f_h(t, a)$ revealing the geometry distribution, the time varying large deviation spectrum $f_g(t, a)$ revealing the probability statistic distribution, and the time varying Legendre multifractal spectrum $f_l(t, a)$.

3.1. Time-varying Hausdorff singularity spectrum distribution

Among the three time-varying singularity spectra, $f_h(t, a)$ possesses the strictest geometry sense and mathematical basement. According to anisotropies hypothesis, the statistic character of stochastic process can be obtained by the sampling signal, so the local character of $x(t)$ can be acquired by $s(t, \tau)$. $s(t, \tau)$ describes the singularity distribution in t, and if $E^{[a]}(t)$ is the point subset with the same singularity exponent in t, then

$$E^{[a]}(t) := \{\tau : \liminf_{n\to\infty} h_{kn}^{(n)}(t) = a\}. \tag{3.1}$$

Research indicates that the Lebesgue measures of these sets are zero,and the set functions describe the relative size, which can be regarded as the spectrum distribution of the set. The sets $E^{[a]}(t)(a \in \Re)$ form a multifractal decomposition of the support of $r_{xx}(t, \tau)$, i.e., they are disjoint and their union is the support of $r_{xx}(t, \tau)$. We will loosely address $r_{xx}(t, \tau)$ as time-varying multifractal if this decomposition is rich, i.e. if the sets $E^{[a]}(t)(a \in \Re)$ are highly interwoven or even dense in the support of $x(t)$.

Definition 3.1. The time-varying Hausdorff spectrum is the function $(t, a) \mapsto \dim(E^{[a]}(t))$, where $\dim(E)$ denotes the Hausdorff dimension of the set E.

The sets $E^{[a]}(t)(a \in \Re)$ give the multifractal decomposition of signal $x(t)$, i.e., the fractal sets with α structure the support of $x(t)$ in t. $\dim(E^{[a]}(t))$ reveals the geometry distribution of singularity exponents. In view of mathematic and statistic analysis, limited covering and measurability of sets, one can get the mathematic expression of $\dim(E^{[a]}(t))$.

Set x is any subset with topology dimension d, μ is a measure on X, and $r_{xx}(t, \tau)$ is the instantaneous self-correlation of $x(t)$. Decompose iteratively (r_{xx}, μ) with α in t, and after n steps, the cells with same measure $\mu_t(\alpha)$ structure the subset $x_t(n, \alpha)$. If $\lim_{n\to\infty} x_t(n, \alpha) = x_t(\alpha)$ is a fractal set, then $x_t(\alpha)$ is called a fractal subset distribution in t,further $r_{xx}(t, \tau)$ is the set sum of fractal subsets $x_t(\alpha)$ with different dimension.

Suppose the cell measure $\mu_t(\alpha)$ and cell ε satisfy power law : $\mu_t(\alpha) \sim \varepsilon^{\alpha}$, α is the Holder exponent or singularity exponent, which controls the singularity of $\mu_t(\alpha)$. For the any δ-covering $\{U_i\}_{i\in N}$ of $x_t(\alpha)$, when $0 < \mathrm{diam}U_i < \delta$, introduce the definition

$$H_\delta^r(x_t(\alpha), \mu_t(\alpha)) = \inf\left\{\sum_{i=1}^{\infty}(\mathrm{diam}U_i)^r : x_t(\alpha) \subset \bigcup_{i=1}^{\infty} U_i\right\}. \tag{3.2}$$

Hereby, the time-varying r dimension Hausdorff measure of $x_t(\alpha)$:

$$H^r(x_t(\alpha), \mu_t(\alpha)) = \lim_{\delta\to 0} H_\delta^r(x_t(\alpha), \mu_t(\alpha)). \tag{3.3}$$

Suppose there exists critical exponent $f_h(t, \alpha)$, which satisfies

$$H^r(x_t(\alpha), \mu_t(\alpha)) = \begin{cases} 0 & r > f_h(t, \alpha) \\ \infty & r < f_h(t, \alpha) \\ \text{Limited number}, & r = f_h(t, \alpha). \end{cases} \tag{3.4}$$

Then $f_h(t, \alpha)$ is the time-varying singularity spectrum in the Hausdorff measure with varied α, and one has time-varying Hausdorff singularity spectrum $f_h(t, \alpha)$, which is exactly the Hausdorff dimension of $x_t(\alpha)$

$$f_h(t, \alpha) = \inf\left\{r : \liminf_{\delta\to 0}\sum_{i=1}^{\infty}(\mathrm{diam}U_i)^r = 0\right\} = \sup\left\{r : \liminf_{\delta\to 0}\sum_{i=1}^{\infty}(\mathrm{diam}U_i)^r = \infty\right\}. \tag{3.5}$$

When $\{U_i\}_{i\in N}$ are all the ε-boxes and the counting of boxes with measure $\mu_t(\alpha)$ in $[\alpha, \alpha + d\alpha]$ is $N_t(\alpha)$, without loss of generality and allowing for arbitrariness of the covering set, there exists

$$H_\varepsilon^r(x_t(\alpha), \mu_t(\alpha)) = N_t(\alpha)\varepsilon^r. \tag{3.6}$$

When $N_t(\alpha) \sim \varepsilon^{-f(t,\alpha)}$, $H_\varepsilon^r(x_t(\alpha), \mu_t(\alpha))$ is limited, and $f_h(t, \alpha) = -\lim_{\varepsilon\to 0} \ln N_t(\alpha)/\ln\varepsilon$.

3.2. Time-varying large deviation spectrum distribution

Large deviation spectrum $f_g(t, a)$ is a comparison between the computation precision and calculation quantity. Eq. (3.6) analyzes the differential interval of singularity exponent, it is too complicated for real calculations. According to the large deviation theory (Gartner–Ellis),the time varying singularity exponent with t behaves as

$$N^{(n)}(a, \varepsilon, t) = \#\{k = 0, \ldots, 2^{n-1} : a - \varepsilon \leq s_k^{(n)}(t) < a + \varepsilon\}. \tag{3.7}$$

Note that $\varepsilon > 0$ is the length of intervals, and $N^{(n)}(a, \varepsilon, t)$ is the number of $s_k^{(n)}(t)$ in the interval $a - \varepsilon$.

Definition 3.2. The time varying large deviation spectrum

$$f_g(t, a) = \lim_{\varepsilon \to 0} \limsup_{n \to \infty} \frac{\log N^{(n)}(a, \varepsilon, t)}{n \log 2}, \tag{3.8}$$

where *sup* is the supremum. $N^{(n)}(a, \varepsilon, t)$ can be considered as the measure with t, and $f_g(t, a)$ is the double limit value when $N^{(n)}(a, \varepsilon, t)$ is constructed as a function of scale 2^{-n}. When substituting sup as inf., one has

$$\underline{f}(t, a) = \lim_{\varepsilon \to 0} \liminf_{n \to \infty} \frac{\log N^{(n)}(a, \varepsilon, t)}{n \log 2}. \tag{3.9}$$

This approach has grown out of the difficulties involved with computation of Hausdorff dimensions, using uniformity coverings instead of optimal coverings in $\dim(E^{[a]}(t))$. In fact $N^{(n)}(a, \varepsilon, t)$ may be used to estimate box dimensions, and in the sense, one has $f_h(t, a) \leq f_g(t, a)$.

3.3. Time varying Legendre multifractal spectrum distribution

$f_l(t, a)$ is developed on the basis of $f_l(a)$. In fact, $f_l(t, a)$ can be labeled as the implementation of a large deviation principle. To this end we consider $N^{(n)}(a, \varepsilon, t)/2^n$ to be the probability to find (for a fixed realization of $r_{xx}(t, \tau)$) a number in t such that $h_{k_n}^{(n)}(t) \in [a - \varepsilon, a + \varepsilon]$, i.e. $P(s_k^{(n)}(t) \in [a - \varepsilon, a + \varepsilon]) = N^{(n)}(a, \varepsilon, t)/2^n$. Typically, there will be one expected or most frequent value of $\lim_{n \to \infty} s_k^{(n)}(t) = \hat{a}(t)$, denoted $\hat{a}(t)$, and $f(t, a)$ will reach its maximum at $a(t) = \hat{a}(t)$, which is the box-counting dimension. If α differs from $\hat{a}$, on the other hand, then $[a - \varepsilon, a + \varepsilon]$ will not contain $\hat{a}(t)$ for small ε and the probability to observe $s_{k_n}^{(n)}$ lying in $[a - \varepsilon, a + \varepsilon]$ will decrease with exponential decaying rate.

Appealing to the theory of the large deviation principle (LDP), one can get "exponential decay rate" $f_l(t, a)$. Consider the random variable $A_n = -ns_{kn}^{(n)}(t) \ln(2)$ where K is randomly selected from $\{0, \ldots, 2^{n-1}\}$ with uniform distribution Un. Introduce its logarithmic moment generating function:

Definition 3.3. For all $q \in R$ the partition function of a path of X is defined as

$$S^{(n)}(t, q) := \sum_{k=0}^{2^n - 1} \exp(-qnh_K^{(n)}(t) \ln(2)) = \sum_{k=0}^{2^n - 1} 2^{-nqh_K^{(n)}(t)}. \tag{3.10}$$

Usually, when $n \to \infty$, $S^{(n)}(t, q)$ follows a power law against 2^{-n}, i.e. $S^{(n)}(t, q) \sim 2^{-n\tau_t(q)}$, where $\tau_t(q)$ is called the time varying scale exponent or mass exponent function. When a limitation exists as $n \to \infty$, one has

$$\tau_t(q) := \liminf_{n \to \infty} -\frac{1}{n} \log_2 S^{(n)}(t, q). \tag{3.11}$$

For certain t, the time series $x(t)$ is the stationary multifractal signal if $\tau_t(q)$ is linear function of q, and $x(t)$ is nonstationary multifractal signal if $\tau_t(q)$ is nonlinear function of q.

According to LDP theory, $N^{(n)}(a, \varepsilon, t)/2^n$ satisfies the LDP's condition and has frequency function $f_l(t, a)$, and we can get the relationship between $\tau_t(q)$ and $f_l(t, a)$. From the partition function, we can study the inner relationship between the mass exponent and Legendre spectrum. In fact, the double limits in the wavelet spectrum are hard to handle. By the way of the partitions function, the double limits can be converted to one limit.

Fix $q \in R$. Let $\gamma < f(a)$ and $\varepsilon > 0$. Then, there are arbitrarily large n such that $N^{(n)}(a, \varepsilon, t) \geq 2^{n\gamma}$. For such n, we have

$$S^{(n)}(t, q) = \sum_{k=0}^{2^n - 1} 2^{-nqh_K^{(n)}(t)} = \sum_{|h_K^{(n)}(t) - a| < \varepsilon} 2^{-nqh_K^{(n)}(t)} \geq N^{(n)}(a, \varepsilon, t) 2^{-n(qa + |q|\varepsilon)} \geq 2^{-n(qa - \gamma + |q|\varepsilon)}.$$

Hereby, $\tau_t(q) \le qa - \gamma + |q|\varepsilon$. Letting $\varepsilon \to 0$ and $\gamma \to f_l(t,a)$, we find $\tau_t(q) \le qa - f_l(t,a)$ and $\tau_t(q) = \sup_{0\le a<\infty}\{qa - f_l(t.a)\}$. Suppose when $a = a(q) > 0$, $\tau_t(q)$ has the maximum value, that is $\frac{d}{da}(f_l(a) - qa)\big|_{a=a(q)} = 0$, and then $q = \frac{df(a(q))}{da}$, which indicates that when the slope of $f_l(t,a)$ is t, $\alpha = \alpha(t,q)$, and we have

$$\tau_t(q) = qa(t,q) - f_l(t,a(q)). \tag{3.12}$$

If the function α of q is differential, then $\frac{d\tau}{dq} = \frac{df}{da}\cdot\frac{da}{dq} - a - q\frac{da}{dq}$, substitute $a = a(t,q)$, we have

$$a(t,q) = -\frac{d\tau_t(q)}{dq}. \tag{3.13}$$

Eqs. (3.12) and (3.13) are the Legendre transform pair in essence,which found the relation between $f_l(t,a)$ and $\tau_t(q)$. In other words, $f_l(t,a)$ can be obtained by the Legendre transform

$$f_l(t,a(t,q)) = qa(t,q) - \tau_t(q), \tag{3.14}$$

which is called the time-varying Legendre multifractal spectrum. $f_l(t,a)$ is a smooth upper concave function, which can be depicted by q. Especially, when $q = 0$, $a(t,q)$ corresponds to the maxima value of $f_l(t,a)$, i.e., $f(t,a(0)) = -\tau_t(0) = D(0)$, which is the box-counting dimension curve of the supported measure. When $q = 1$, $df_l(t,a(1))/da = 1$ and $f_t(a(1)) = a(1) - \tau_{t,(1)}$, due to $\tau_t(1) = 0$, one has $f_l(t,a(1)) = a(t,1) = -d\tau_t(1)/dq = \lim_{\delta\to 0}\sum_i \mu_{B_i}(\delta)\ln\mu_{B_i}(\delta)/\ln\delta$, i.e., the information dimension curve, where the slope of f_l is equal to 1.

Proposition 3.4. *For all $q \in R$, if the limit $\tau(t,q) := \lim_{n\to\infty} -\log_2 S^{(n)}(t,q)/n$ exists, and $\tau(t,q)$ is the differential function of q, then the double limit $f_l(t,a) = \lim_{\varepsilon\to 0}\lim_{n\to\infty}\log_2 N^{(n)}(a,\varepsilon,t)/n$ exists, and one has*

$$f_l(t,a) = \underline{f}(t,a) = \tau^*(t,a) := \inf_{q\in R}(qa - \tau(t,q)); \qquad a_t = \frac{d\tau_t(q)}{dq} \quad \text{for all } \alpha, \tag{3.15}$$

where $\tau^*(\cdot)$ is the Legendre transform, and $\tau^*(t,a)$ is the time varying Legendre spectrum. f_h is the geometry distribution of the singularity structure. f_g is the probability distribution and f_l is a compromised value, adapted to calculation, which satisfies the inequality $f_h(t,a) \le f_g(t,a) \le f_l(t,a)$. For most applications, the above hypothesis is too strict, and in the real applications, the time-varying multifractal spectrum is too hard to handle. Due to the complexity and diversity of the algorithm, the reliability of output is terrible, so the computation simulation of the time-varying quadratic multifractal spectrum distribution based on WTMM is an efficient and common method.

4. The quadratic time-varying singularity spectrum distribution based on WTMM

The above three kinds of calculation methods of multifractal spectrum are based on the singularity matrix, which is deduced as the Holder exponent and wavelet singularity exponent. Compared with the Holder exponent, the wavelet singularity exponent is reliable and adapt to calculation, and research indicates that for fractals the multi-scales wavelet analysis has three advantages: (1) Wavelet transform has strong scanning and tracking ability for a singular point,while it is blind to the regular points,which can overlook amounts of redundancy information. (2) The regularity of signal can be characterized completely by the wavelet maxima lines, and in the time and scale domains plane, there is at least one wavelet maxima line pointing towards each singular point, when the Holder exponent is less than the vanished moment of the wavelet. (3) Wavelets can be looked as "generalized oscillating boxes", and the wavelet transform is an adaptive covering of the signal, and wavelet boxes possess the character of self-adaptive space/time/scale separation for fractals.

Hereby, instead of using the wavelet singularity exponent directly, based on the WTMM and the time varying Legendre multifractal spectrum, one has the quadratic time varying singularity spectrum distribution on WTMM.

4.1. Times-singularity spectrum distribution based on WTMM

The quadratic time varying singularity spectrum distribution on WTMM utilizes the advantage of wavelet, and tracking the exponential law of decrease along the wavelet maxima lines, which is formed from the local maxima value of wavelet coefficient at each scale. The time varying singularity spectrum distribution on WTMM is showed as a feasible method, which in essence is the Legendre multifractal based on wavelet singularity exponent, but it differs from the definition of Section 3.3.

Firstly the wavelet transform of the instantaneous self-correlation of signal

$$Wf_t(a,x) = \frac{1}{a}\int x(t+\tau/2)x^*(t-\tau/2)\psi\left(\frac{\tau - x}{a}\right)\mathrm{d}\tau. \tag{4.1}$$

As Arneodo proposed, the partition function

$$S_t(a,q) = \int_R |Wf_t(a,x)|^q\,\mathrm{d}x. \tag{4.2}$$

As in the above analysis, substitute the continuous integral of wavelet coefficient for the discrete sum, and then define $L(a_0)$ as the set of maxima lines at scale α, which satisfies

$$(a, x) \in l \Rightarrow a \leq a_0, \quad \text{and} \quad \forall a \leq a_0, \exists (a, x) \in l.$$

The partition function based on $L(a_0)$ is

$$S_t(a, q) = \sum_{l \in L(a)} \left[\sup_{\substack{(a', x) \in l \\ a' \leq a}} \left| Wf_t(a', x) \right| \right]^q. \tag{4.3}$$

Eq. (4.3) shows that $S_t(a, q)$ is similar to the traditional partition function: the analyzed wavelet is a special box, the size of box is α, and location of box is decided to the maxima line. The supremum of the wavelet module maxima eliminates the instability and surge in numbers of $S_t(\alpha, q)$ due to the small coefficient and oscillation fast around the maxima value. Furthermore, for the binary discrete wavelet transform, given $\psi_{j,k}(k) = 2^{j/2}(2^j t - k)$ with vanishing moment R, the wavelet transform of the instantaneous self-correlation signal

$$W_{j,k} = \int x(t + \tau/2) x^*(t - \tau/2) \psi_{j,k}(t) d\tau.$$

For large j, $W_{j,k}$ contained the small scale and high frequency information, while for small j, $W_{j,k}$ contained the coarse scale and low frequency information, and then the partition function is

$$T_t(j, q) = \sum_{l \in L(j)} \left[\sup_{\substack{(j', k) \in l \\ j' \leq j}} |Wf_t(j, k)| \right]^q. \tag{4.4}$$

Asymptotic decaying rate of $S_t(a, q)$ over scale a is measured by the scale exponent $\tau(t, q)$. When scale $a \to 0$, $S_t(a, q) \sim a^{\tau(t,q)}$, then one has the time varying mass function:

$$\tau(t, q) = \frac{\log S_t(a, q)}{\log a}. \tag{4.5}$$

Through the Legendre transform, one has

$$f_l(t, a(t, q)) = qa(t, q) - \tau_t(q); a(t, q) = -\frac{d\tau_t(q)}{dq}. \tag{4.6}$$

4.2. Implementation of the time-varying wavelet transform modulus maxima

4.2.1. Wavelet type

The applied wavelet function can be any one with the number of vanishing moments that are one degree higher than the highest vanishing moment of the signal. As it is mentioned, the applied wavelet can be the derivatives of the Gaussian function, such as the first derivative of Gaussian (DOG1), or second derivative of Gaussian (DOG2). It should be noted that the DOG1 and DOG2 are pseudo wavelets because they have infinite support rather than a compact support. However, since their tails converge to zero very fast, they can be used as wavelets. There are two major advantages in using this family of wavelets: (i) it is possible to achieve arbitrary large vanishing moment m by calculating the mth derivative of the Gaussian, and (ii) they have simple mathematical formulae for the Fourier transform.

4.2.2. Selection of the scales

Since the fractal signals of interest are discrete and finite in size, their range of scales cannot be taken from zero to infinity. Since in the computation of mass function, logarithmic behavior of the scales is of interest, scales are selected such that their log plot constructs a line. For a finite sized signal, the best achievable resolution is 1 sample. Thus, for a signal with K samples, the finest achievable scale is K, and the coarsest achievable scale is 1. For the time varying wavelet transform modulus maxima, the selection of the scales can vary according to the different time to ensure the linearity of the plot between $\log S_t(a, q)$ and $\log a$, especially when the singularity spectra diverge in a wide scope.

4.2.3. Selection of the moment q

Theoretically, the finer the interval of q is, the more accurate $a(t, q)$ is due to the limited differential. Furthermore, the selection of $q_{\min}$ and $q_{\max}$ should ensure the existence of q-order moment of wavelet coefficient. But in the practical application of TS-MFSD, the cost of quantity is enormous, because the selection of q influences the structure of partition function $S_t(a, q)$ and mass function $\tau(t, q)$. Based on roughly estimation, when the interval of q increases N times, the cost of quantity will increases $4N$ times approximately. Furthermore, the selection of q can vary according to the different time of the time-varying wavelet singularity exponent. For example, the interval and scope of q can be selected constantly for the mono-fractal signal, and should be selected diversely for the non-stationary multifractal signal according to the characteristic of signal. From the Eq. (4.6), singularity exponent is the derivation of $\tau_t(q)$. Thus, to obtain the matrix $f(t, a)$, a uniform interval and scope of singularity exponent in a different time should be got by the interpretation of q.

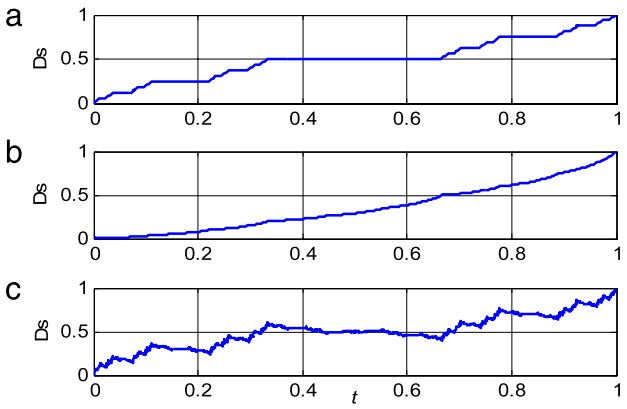

Fig. 1. The Devil's Staircase signal with (a) $p1 = 0.5$, $p2 = 0$, $p3 = 0.5$, (b) $p1 = 0.2$, $p2 = 0.3$, $p3 = 0.5$, and (c) $p1 = 0.6$, $p2 = -0.2$, $p3 = 0.6$.

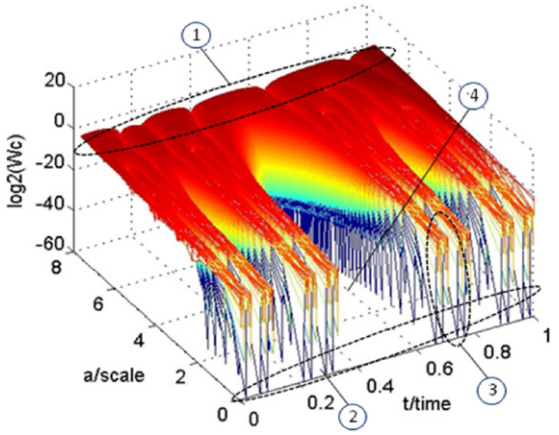

Fig. 2. The WTMM of the quadratic Devil's Staircase signal with $p1 = 0.5$, $p2 = 0$, $p3 = 0.5$ at given delayed time, and the four regions represent different singularity characteristics and origins of the signal.

5. Experimental results and discussion

5.1. Numerical series: Devil's Staircase signal

In order to test the validity of TS-MFSD, the multifractal signal selected for experiments is the Devil's Staircase (DS) signal for the Cantor set with different weight, as shown in Fig. 1. In general, there are two types of DS: monotonic (Fig. 1(a), (b)), and non-monotonic (Fig. 1(c)).

Fig. 2 shows the wavelet transform module of signal (a), and it provides a surface representation of the matrix in the log–log-linear scale. The parameters $\log_2 W_c$ and $\log_2 s$ are dimensionless. Region ① in Fig. 2 shows that the amplitude of W_c at the coarsest scales is higher than the finest scales over t. Fig. 2 also shows that the amplitude of W_c at the very fine scales decreases significantly. The coefficients of region ② in Fig. 2 are very small, and when this region is compared to its representation in Fig. 3, these coefficients are not actual extensions of the maxima lines. Consequently, these coefficients are due to numerical noise, not the actual singularities. On the other hand, region ③ shows the coefficients that are due to the actual singularities. Such coefficients are at the extension of the maxima lines, decay slowly, and are more organized. In Fig. 2, region ④ shows that for the neighborhood of $t = 0.5$, the coefficients are very small and they are disconnected from the maxima lines. Thus, these coefficients are due to computational errors, not due to the singularities.

Fig. 3(a) shows the WTMM line in the time and scale plane. In order to construct the maxima lines, singularity points across the scales are tracked and chained into a maxima line, as shown in Fig. 3(a). The maxima points of the successive scales are close to one another, and can be tracked. Each maxima line can be tracked from the coarsest scale to the very fine scales. It should be noted that all maxima lines which are not continuing down to very fine scales are dismissed from the computation of the partition function. Fig. 3(b) shows the time varying Legendre multifractal spectrum distribution of the quadratic signal (a), where the singularity spectrum was changed along the time. From the experiment of devil staircases, we can see that the time-singularity multifractal spectrum (TS-MFSD) describes the time-varying singularity distribution, which indicated the spatial dynamics character of system.

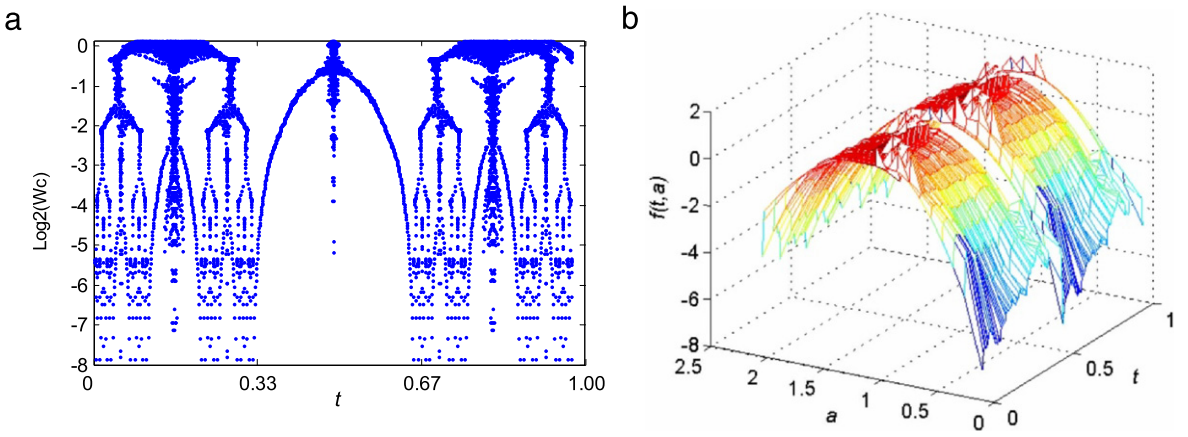

Fig. 3. (a) The WTMM line of the Devil's Staircase signal at given delayed time, where the singularity points across the scales are tracked and chained into a maxima line from coarse scales to the very fine scales, and the branching and bifurcation can be easily observed, and (b) the time varying Legendre multifractal spectrum distribution of the Devil's Staircase signal with $p1 = 0.5$, $p2 = 0$, $p3 = 0.5$.

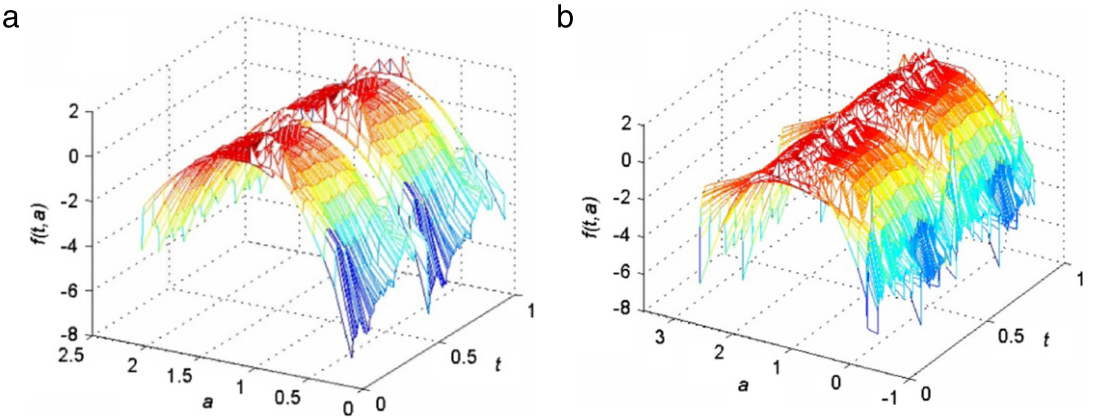

Fig. 4. The time varying Legendre multifractal spectrum distribution of the Devil's Staircase signal with (a) $p1 = 0.2$, $p2 = 0.3$, $p3 = 0.5$, where the maximum of multifractal spectrum is near 1, and the singularity spectra at different time have the similar characteristic along the time, except around $t = 0.5$, and (b) $p1 = 0.6$, $p2 = -0.2$, $p3 = 0.6$, where the spectrum is more complex than the (a) and the singularity scope is wider than (a), which indicates signal (b) possesses a more complicated fractal characteristic than signal (a).

The Fig. 4(a) shows the time varying Legendre multifractal spectrum distribution of the Devil's Staircases signal (b), and Fig. 4(b) shows the time varying Legendre multifractal spectrum distribution of the Devil's Staircase signal (c). The Fig. 5(a) shows the time-varying large deviation multifractal spectrum of the Devil's Staircase signal (b), and Fig. 5(b) shows the time-varying large deviation multifractal spectrum of the Devil's Staircase signal (c). For given time, the TS-MFSD $f_g(t, a)$ or $f_l(t, a)$ is a convex function and has a maxima value equal to 1, and as time goes, the MFS evolves along, which indicates that TS-MFSD is an extension of MFS and is more efficient than the latter.

Besides, there are two points worth to be pay attention. Firstly, there are some time intervals, such as $t \in [0.45, 0.55]$, the spectrum distribution is translated into spectrum line, which indicated that there is weak fractal characteristic there. Secondly, Figs. 4 and 5 appear the strong fringe effect, which lead to the distortion of MFS there. In addition, from the experiment of Devil's staircase, we can see that the time-varying multifractal spectrum describe the dynamics evolving process of MFS of non-stationary signal, and the time-singularity multifractal spectrum distribution indicates the spatial dynamics character of system. Experiments also show that f_g and f_l are consistent with f_h and they satisfy approximately the inequality $f_h(t, a) \leq f_g(t, a) \leq f_l(t, a)$. The above calculation is elementary and a further study will elaborate on the algorithm of time-varying multifractal spectrum based on the WTMM.

5.2. Multifractal synthesis by fraclab: Multifractional Brownian motion

Here, the stochastic Multifractional Brownian Motion (mFBM) synthesized by Fraclab2.05 in Matlab2010 is studied. The mFBM is implemented as linear singularity modulation, and the local Holder exponent $H(t) = 0.1 + 0.8t$, $t \in [0, 1]$.

The sample size of mFBM is 512, and Fig. 6(a) is the linear mFBM signal, Fig. 6(b) is the multifractal spectrum based on WTMM method, and Fig. 6(c) is the time-singularity multifractal spectrum based on the WTMM, which indicates that the

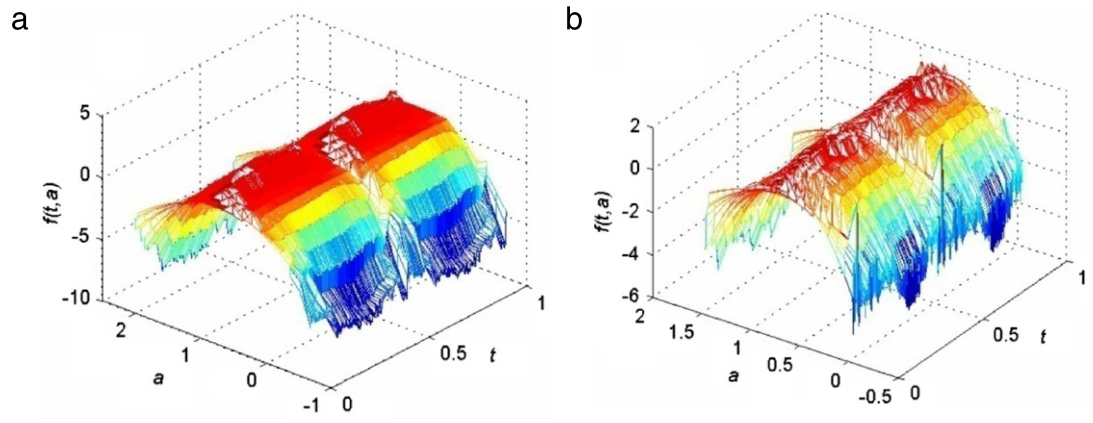

Fig. 5. The large deviation multifractal spectrum distribution of the Devil's Staircase signal with (a) $p1 = 0.2$, $p2 = 0.3$, $p3 = 0.5$, and (b) $p1 = 0.6$, $p2 = -0.2$, $p3 = 0.6$, which have similar spectra with the time varying Legendre multifractal spectrum distribution in spite of the quantity divergence.

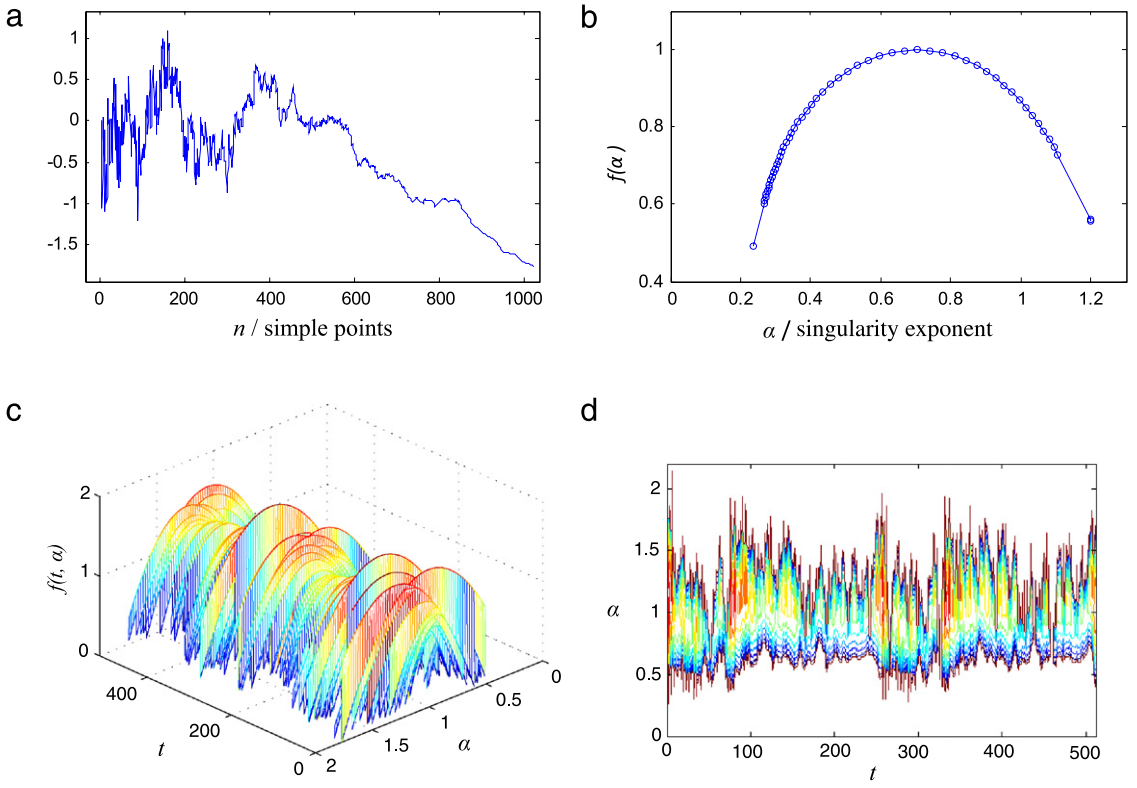

Fig. 6. The simulation analysis of fractal characteristic of the linear singularity modulation mFBM with $H = 0.1 + 0.8t$; (a) the linear mFBM signal; (b) the multifractal spectrum; (c) the time singularity multifractal spectrum based on the WTMM method, and (d) the contour line of the TSMFSD of mFBM, the wider the singularity of signal is, the stronger the intensity of singularity is.

mFBM possesses multifractal characteristic at any time and represents the concave fractal spectrum, but the multifractal spectra vary stochastically along the time. Fig. 6(d) is the contour of the Fig. 6(c). We can see that the width of singularity varied along with the time axis. In some time intervals, the width of singularity is small, which implies the singularity characteristic is weak, and in others, there are a few blank strips, which implies these points are ordinary. Calculate the singularity range $\Delta a(t) = a_+(t) - a_-(t)$, where $a_+(t)$ is the maxima of singularity at t, and $a_-(t)$ is the minima of singularity at t. $\Delta a(t)$ indicates the intension of singularity along with t. We can also calculate the singularity curve corresponding to the maximal multifractal spectrum, i.e., $a_m(t) = \arg_a \max f(t, a)$, and $a_m(t)$ tracks the evolvement of singularity along with time (see Fig. 6).

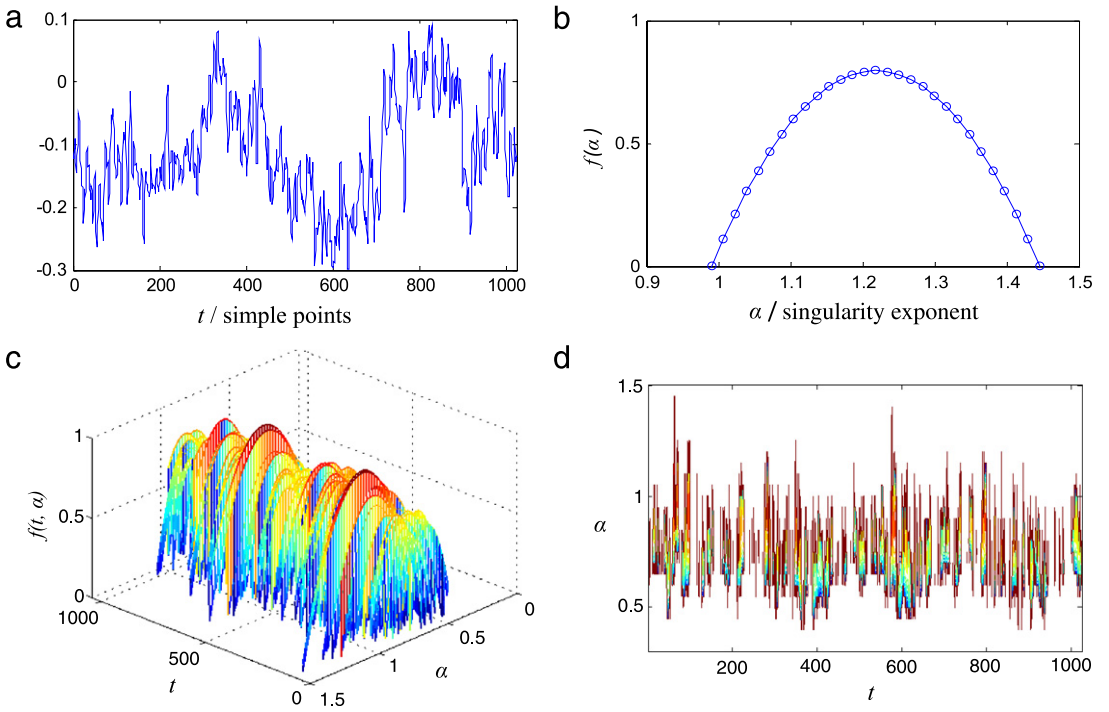

Fig. 7. The simulation analysis of TSMFSD of the sea clutter. (a) the sea clutter with 2^{10} points; (b) the multifractal spectrum of sea clutter; (c) the time singularity multifractal spectrum based on the WTMM method, and (d) the contour line of the TSMFSD of sea clutter, the wider the singularity of signal is, the stronger the intensity of singularity is.

5.3. Natural data: Sea clutter from the ocean radar

Finally, we analyze the natural series corresponding to sea clutter from the ocean radar, applying the time-singularity multifractal spectrum method. The sea surface is a kind of multi-measurement fractal surface, and the angle distribution of the scattering energy preserves the spatial fractal character of the sea surface after the reciprocity between electromagnetic wave and the fractal surface. We have lots of evidence of the multifractal behavior of the sea clutter signal from ocean radar [34,35]. The actual data were gathered from the radio ocean radar. The altitude of the radar beyond the sea was 10–25 m. The signal frequency of the carrier frequency was 150 MHz, and the echoed signal was through two channels: the frequency demodulation channel and the amplitude demodulation channel. The demodulated data of amplitude channel and frequency channel were sampled with 50 kHz. Here, we take sea clutter data with 2^{10} points and analyze the TSMFD characteristic.

The sea clutter is shown in Fig. 7(a), where the high frequency component has little variance while the low frequency component has the high variance. Fig. 7(b) is the multifractal spectrum based on WTMM method, and Fig. 5(c) is the time-singularity multifractal spectrum distribution based on the WTMM, which indicates that the sea clutter possesses multifractal characteristic almost everywhere and represents the concave fractal spectrum distribution. At the same time, the multifractal spectra vary stochastically along the time, and there are some blank strips in the TSMFSD, which is evident in the Fig. 7(d). The blank strips indicate that there exist some time intervals without fractal characteristic.

It should be noted that the physical meaning of TS-MFSD and the characteristic of $f(t, a)$ in given time or singularity are in a puzzle. In addition, we should pay attention to the fringe effect and the calculation quantity of TS-MFSD, which imprison the engineering application of TS-MFSD. However, these problems could be solved if we consider the short time series and adopt the DFA-MFA method, which have less calculation quantity.

6. Conclusion

In this paper, we proposed the time-singularity multifractal spectrum distribution (TS-MFSD), which involves time-varying Hausdorff singular spectrum distribution, time-varying large deviation multifractal spectrum and time-varying Legendre spectrum distribution, which exhibit the singularity exponent distribution of a fractal signal at arbitrary time. We studied times-singularity spectrum distribution based on the Wavelet Transform Module Maxima (WTMM) Method, and proposed the algorithm of the TS-MFSD based on the WTMM, analyzed the implementation of the time varying wavelet transform modulus maxima, including the wavelet type, selection of the scales, selection of the moment and the thresholding the maxima.

Furthermore we discussed the characteristic of TS-MFSD based on a Devil's Staircase signal, stochastic fractional motion and real sea clutter. From the experiment, we conclude that: (1) TS-MFSD is the extension of MFS and more efficient than the latter, and for given time, the TS-MFSD $f(t, a)$ is a convex function with maxima value 1, which indicates the point spectral characteristic and the evolving law of the multifractal signal. It is hoped that we can reveal the dynamics evolving process and the spatial dynamics character of fractal nonlinear system. (2) Moreover, we find that there are some time intervals in the TS-MFSD, the two-dimensional spectrum distribution is translated into a spectrum line caused by the mono-fractal or the non-fractal point of the signal, and it satisfied the Multifractal spectrum (MFS), where the MFS is translated into a single point. (3) From the experiment, we also believe that f_g and f_l are consistent with f_h and they satisfy the inequality $f_h(t, a) \leq f_g(t, a) \leq f_l(t, a)$ for given time, just as $f_h(a) \leq f_g(a) \leq f_l(a)$ in the MFS.

Further studies will concentrate on the physical meaning of TS-MFSD, the characteristic of $f(t, a)$ in given time or singularity, the TS-MFSD of natural fractal signal in the real world and the TS-MFSD based on the DFA-MFA and the WL, according to the discussion.

Acknowledgments

We would like to thank Prof. H. c. Zhao of Nanjing University of S&T and Prof. X. n. Yang in CETC for their support and encouragement towards the research, and hui Zhao for manuscript revisions. We are grateful to the anonymous reviewers for valuable comments and suggestions.

This work was partially supported by the National Science Research Foundation of China (NSFC, Grant Number 61171168 and 60702016).

References

[1] B.B. Mandelbrot, A multifractal walk down wall street, Scientific American 280 (1999) 70–73.
[2] H.E. Stanley, L.A. Amaral, P. Gopikrishnan, P.Ch. Ivanov, T.H. Keitt, V. Plerou, Scale invariance and universality: organizing principles in complex systems, Physica A 281 (2000) 60–68.
[3] Y. Ashkenazy, P.Ch. Ivanov, S. Havlin, Ch.-K. Peng, A.L. Goldberger, H.E. Stanley, Magnitude and sign correlations in heartbeat fluctuations, Physical Review Letters 86 (9) (2001) 1900–1909.
[4] L. Telesca, V. Lapenna, M. Macchiato, Multifractal fluctuations in seismic interspike series, Physica A 354 (2005) 629–640.
[5] L. Zunino, B. Tabak, A. Figliola, D.G. Perez, M. Garavaglia, O.A. Rosso, A multifractal approach for the stock market inefficiency, Physica A 387 (2008) 26–37.
[6] L. Pietronero, E. Tosatti, Fractals in Physics, North-Holland, Amsterdam, 1986.
[7] K. Falconer, Techniques in Fractal Geometry, John Wiley and Sons Ltd., New York, 1997.
[8] K. Falconer, Fractal geometry, in: Mathematical Foundations and Applications, John Wiley and Sons Ltd., Chichester, 1990.
[9] H.E. Stanley, N. Ostrowsky, On Growth and Form: Fractal and Non-Fractal Patterns in Physics, Nijhoff, Dordrecht, 1985.
[10] P. Grassberger, On the Hausdorff dimension of fractal attractors, Journal of Statistical Physics 26 (1981) 173–179.
[11] P. Grassberger, Procaccia measuring the strangeness of strange attractors, Physica D 9 (1983) 189–208.
[12] P. Grassberger, Estimating the fractal dimensions and entropies of strange attractors, Chaos 1 (1986) 291–311.
[13] A. Chhabra, R. Jensen, Direct determination of the $f(\alpha)$ spectrum, Physical Review Letters 62 (12) (1989) 1327–1330.
[14] A. Chhabra, C. Maineveau, R. Jensen, K.R. Sreenivasan, Direct determination of the $f(\alpha)$ spectrum and its application on fully develop turbulence, Physical Review A 409 (1989) 5284–5294.
[15] J.F. Muzy, E. Bacry, A. Arneodo, Wavelets and multifractal formalism for singular signals: application to turbulence data, Physical Review Letters 67 (1991) 3515–3518.
[16] E. Bacry, A. Arneodo, J.F. Muzy, Singularity spectrum of fractal signals from wavelet analysis: exact results, Journal of Statistical Physics 70 (1993) 635–674.
[17] A. Arneodo, A. Argoul, J.F. Muzy, M. Tabard, E. Bacry, Beyond classical multifractal analysis using wavelets: uncovering a multiplicative process hidden in the geometrical complexity of diffusion limited aggregates, Fractals 1 (1995) 629–646.
[18] C.K. Peng, S.V. Buldyrev, A.L. Goldberger, S. Havlin, R.N. Mantegna, M. Simons, H.E. Stanley, Statistical properties of DNA sequences, Physica A 221 (1995) 180–192.
[19] R.B. Govindana, J.D. Wilsona, H. Preil, H. Eswaran, J.Q. Campbell, C.L. Lowery, Detrended fluctuation analysis of short datasets: an application to fetal cardiac data, Physica D 226 (2007) 23–31.
[20] C.-K. Peng, S. Havlin, H.E. Stanley, A.L. Goldberger, Quantification of scaling exponents and crossover phenomena in nonstationary heartbeat time series, Chaos 5 (1995) 82–87.
[21] H.E. Stanley, et al., Anomalous fluctuation in the dynamics of complex systems from DNA and physiology to econophysics, Physica A 224 (1996) 545–552.
[22] C.P. Pan, B. Zheng, Y.Z. Wu, X.W. Tang, Detrended fluctuation analysis of human brain electroencephalogram, Physics Letters A 329 (2004) 130–135.
[23] A. Castro e Siva, J.G. Moreira, Roughness exponents to calculate multi/affine fractal exponents, Physica A 235 (1997) 327–333.
[24] J.W. Kantelhardt, S.A. Zschiegner, E. Koscielny-Bunde, S. Havlin, A. Bunde, H.E. Stanley, Multifractal detrended fluctuation analysis of nonstationary time series, Physica A 316 (2002) 87–114.
[25] P. Oswiecimka, J. Kwapien, S. Drozdz, Wavelet versus detrended fluctuation analysis of multifractal structures, Physical Review E. 74 (2006) 8–17.
[26] S. Jaffard, Wavelet techniques in multifractal analysis, fractal geometry and applications: a jubilee of Benoit Mandelbrot, in: M. Lapidus, M. van Franken huijsen (Eds.), in: Proceedings of Symposia in Pure Mathematics Providence, 72, AMS, 2004, pp. 91–151. part 2.
[27] B. Lashermes, S. Jaffard, P. Abry, Wavelet leaders in multifractal analysis, in: Proceedings of IEEE International Conference on Acoustics Speech, and Signal, in: IEEE Acoustics Speech and Signal, vol. 4, 2005, pp. 161–164.
[28] S. Jaffard, Some mathematical results about the multifractal formalism for functions, in: C. Chui, L. Montefusco, L. Puccio (Eds.), Wavelets: Theory, Algorithms, and Applications, Academic Press, 1994, pp. 325–362.
[29] S. Jaffard, Multifractal formalism for functions, parts 1: results valid for all functions and part 2: self similar functions, SIAM Journal of Mathematical Analysis 28 (4) (1997) 944–998.
[30] B. Lashermes, S.G. Roux, P. Abry, S. Jaffard, Comprehensive multifractal analysis of turbulent velocity using wavelet leaders, The European Physical Journal B. Condensed Matter and Complex Systems 61 (2) (2008) 201–205.
[31] Aicko Y. Schumann, J.W. Kantelhardt, Multifractal moving average analysis and test of multifractal model with tuned correlations, Physica A 390 (2011) 2637–2654.
[32] A. Bashan, R.P. Bartsch, J.W. Kantelhardt, S. Havlin, Comparison of detrending methods for fluctuation analysis, Physica A 387 (21) (2008) 5080–5090.

[33] J. Alvarez-Ramirez, E. Rodriguez, J.C. Echeverria, Detrending fluctuation analysis based on moving average filtering, Physica A 354 (2005) 199–219.
[34] G. Xiong, X.N. Yang, H.C. Zhao, The Short-Time Multifractal Formalism: Definition and Implement. in: ICIC 2008, CCIS 15, Shanghai, China, 2008. pp. 541–548.
[35] G. Xiong, X.N. Yang, H.C. Zhao, The short-time multifractal spectral analysis based on the singularity exponents, in: IEEE International Conf. on Microwave and Millimeter-Wave Technology, vol. 4, Guilin, China, 2007, pp. 207–210.
[36] Y. Wang, Y.S. Zhu, A short-time multifractal approach for arrhythmia detection based on fuzzy neural network, IEEE Transactions on Biomedical Engineering 48 (9) (2001) 989–995.